The b_{arg36} contributes to efficient coupling in F_1F_O ATP synthase in *Escherichia coli*

Amanda K. Welch · Shane B. Claggett · Brian D. Cain

Abstract In *Escherichia coli*, the F_1F_O ATP synthase *b* subunits house a conserved arginine in the tether domain at position 36 where the subunit emerges from the membrane. Previous experiments showed that substitution of isoleucine or glutamate result in a loss of enzyme activity. Double mutants have been constructed in an attempt to achieve an intragenic suppressor of the $b_{arg36 \rightarrow ile}$ and the $b_{arg36 \rightarrow glu}$ mutations. The $b_{arg36 \rightarrow ile}$ mutation could not be suppressed. In contrast, the phenotypic defect resulting from the $b_{arg36 \rightarrow glu}$ mutation was largely suppressed in the $b_{arg36 \rightarrow glu, glu39 \rightarrow arg}$ double mutant. *E. coli* expressing the $b_{arg36 \rightarrow glu, glu39 \rightarrow arg}$ subunit grew well on succinate-based medium. F_1F_O ATP synthase complexes were more efficiently assembled and ATP driven proton pumping activity was improved. The evidence suggests that efficient coupling in F_1F_O ATP synthase is dependent upon a basic amino acid located at the base of the peripheral stalk.

Keywords F_1F_O ATP synthase · *b* Subunits · ATPase

Introduction

The F_1F_O ATP synthase is the principal enzyme for ATP generation in most organisms. In higher eukaryotes the enzyme is located in the inner mitochondrial membrane, in plants in the chloroplast thylakoid membrane, and in bacteria in the cytoplasmic membrane. The overall structure of the enzyme is highly conserved in all organisms. The F_1

A. K. Welch · S. B. Claggett · B. D. Cain (✉)
Department of Biochemistry and Molecular Biology,
University of Florida,
1600 SW Archer Rd., P.O. Box 100245,
Gainesville, FL 32610, USA
e-mail: bcain@ufl.edu

sector houses catalytic sites for the production of ATP from ADP and P_i (Stock et al. 2000; Boyer 2002; Senior et al. 2002). In bacteria, F_1 consists of nine proteins present in a stoichiometry of $\alpha_3\beta_3\gamma\delta\varepsilon$, with the α and β subunits arranged in an alternating hexamer. The γ and ε subunits form the central, or rotor, stalk that extends up through the middle of the $\alpha_3\beta_3$ hexamer. High-resolution structural analysis of the bovine F_1 sector has shown that each of the catalytic sites exist in different conformations based on interactions with the rotor (Leslie et al. 1999).

The rotational energy of the F_O sector is translated to chemical energy in the F_1 sector (Boyer 1993). In *Escherichia coli*, F_O consists of three subunits present in the ab_2c_{10} stoichiometry. The *a* subunit houses the proton channel. The protons flow through the channel and bind the *c* subunit. Protonation and/or deprotonation of individual *c* subunits drives the rotational movement of the *c* ring, in turn causing rotation of the γ and ε subunits. The function of the peripheral stalk, $b_2\delta$, is to hold F_1 against the movement of the rotor. A high-resolution structure of the bovine peripheral stalk suggests that it bends around F_1 (Dickson et al. 2006). The bacterial *b* subunit has been divided into four functional domains. The membrane-spanning domain consists of the amino terminal 24 amino acids that are largely hydrophobic and responsible for anchoring the *b* subunit in the membrane. The tether domain roughly corresponds to the segment from the top of the membrane to the bottom of F_1. The dimerization domain falls in a highly α-helical polar segment, b_{53-122} (Del Rizzo et al. 2002). The *b* subunits are thought to interact via hydrophobic residues located in this largely polar region (Motz et al. 2004). The F_1 binding domain, $b_{val124-leu156}$, interacts with an $\alpha\beta$ pair and with the δ subunit at the extreme carboxyl terminus (McLachlin et al. 1998; Revington et al. 1999; McLachlin and Dunn 2000;

McLachlin et al. 2000). One of the two b subunits can be crosslinked to the δ subunit without a loss of activity (Ogilvie et al. 1997), providing direct support for the idea that these subunits act as a stator to hold the F_1 sector in place.

The membrane-spanning and tether domains of the b subunits interact with other subunits located within the F_O sector. The transmembrane segments of each b subunit, together with subunits a and c, is the minimum subcomplex required for proton translocation (Greie et al. 2004). Additionally, the b subunits co-purified with a His-tagged a subunit, showing an ab_2 subcomplex within the enzyme (Stalz et al. 2003). Several crosslinking experiments have shown that the a and c subunits interact with the b subunit. The $b_{asn2→cys}$ subunit was crosslinked to cysteine residues introduced at positions 74, 75, and 78 at the carboxyl terminus of the c subunit (Jones et al. 2000). Crosslinking of the two subunits inhibited ATP driven proton pumping, and this was interpreted as the inhibition of the rotation of the c ring (Jones et al. 2000). A site located in the first cytoplasmic loop of the a subunit, $a_{lys74→cys}$, has been crosslinked to the b subunit using a photoactivatable crosslinking agent with little effect on proton translocation (Long et al. 2002). In a similar experiment, the $b_{arg36→cys}$ was found to crosslink to the a subunit (McLachlin et al. 2000).

In the absence of a complete structure of the b subunits, mutational studies have provided the most useful information on the b subunit dimer (Cain 2000). In the membrane-spanning domain, replacement of several amino acids as a group resulted in a loss of function of the enzyme (Hardy et al. 2003). Mutagenesis experiments indicated that the length of the tether region could be manipulated. Functional F_1F_O ATP synthase was obtained using b subunits with insertions of up to 14 amino acids or deletions up to 11 amino acids (Sorgen et al. 1998; Sorgen et al. 1999). The tether domain also contains the b_{arg36} residue that is conserved among bacterial species. Several mutants were constructed to replace b_{arg36}. The $b_{arg36→ile}$ and $b_{arg36→glu}$ substitutions both resulted in a defective F_1F_O ATP synthase and the latter was a true uncoupling mutation (Caviston et al. 1998). The phenotypes of both the $b_{arg36→ile}$ and $b_{arg36→glu}$ mutations could be suppressed by coexpression with a wild type b subunit (Grabar and Cain 2004). The $b_{arg36→lys}$ mutation, however, resulted in a phenotype similar to that of wild-type. Other substitutions allowed limited F_1F_O assembly and enzymatic activity. This suggested that while the b_{arg36} was not essential for function, it did exert an important influence on the enzyme.

The present work further investigates mutations affecting the highly conserved b_{arg36} residue. A series of double mutants were constructed in order to move the arginine residue vertically along the b subunit to consider positional effects for the basic group. Second site substitutions moved

the arginine, replacing either a naturally occurring glutamate or isoleucine. The $b_{arg36→ile}$ mutation could not be suppressed with an arginine located either above or below position 36. However, we present biological and biochemical evidence of a strong intragenic suppressor to the $b_{arg36→glu}$ mutation that restored near normal F_1F_O ATP synthase activity.

Experimental procedures

Materials Molecular biology enzymes and oligonucleotides were obtained from New England Biolabs and Invitrogen, respectively. Reagents were acquired from Sigma-Aldrich and Fisher Scientific. Western blotting reagents and high performance chemiluminescence film were purchased from Amersham Pharmacia Biotech. The monoclonal antibodies against the V5 epitope tag were obtained from Invitrogen. The anti-mouse, horseradish peroxidase linked whole antibody (from sheep), was a product of GE Healthcare, UK Limited.

Mutagenesis, strains and media The wild type b subunit plasmid, pTAM46 (b_{V5}), and the parental mutant plasmids, pTAM54 ($b_{arg36→glu\ V5}$) and pTAM53 ($b_{arg36→ile\ V5}$), that were used to generate the double mutants have been previously described (Grabar and Cain 2004). Site-directed mutagenesis was either performed by a Stratagene Quik-Change kit or by ligation-mediated mutagenesis between the *Mfe*I site and *PpuM*I site (Fig. 1). Plasmids were purified using the Qiagen Mini-Prep and Maxi-Prep kits (Qiagen, Inc.). Restriction endonuclease digestions, ligations, and transformations were conducted according to the recommendations of the manufacturers. Double stranded DNA sequence determinations were performed by either the automated sequencing at the core facility at the University of Florida Interdisciplinary Center for Biotechnology Research or at the Center for Mammalian Genetics. The sequence of the mutagenized region of each plasmid constructed, along with any restriction sites inserted for screening purposes, is shown in Fig. 1.

All recombinant plasmids and the control plasmids: pBR322 (Δb), pTAM46 (b_{V5}), pTAM54 ($b_{arg36→glu\ V5}$), and pTAM53 ($b_{arg36→ile\ V5}$; Grabar and Cain 2004) were expressed in *E. coli* strain KM2 (Δb) so that the only b subunits expressed were that of the plasmid gene (McCormick and Cain 1991). For membrane preparations, strains were grown in Luria broth supplemented with 0.2% (w/v) glucose (LBG). For plate growth, isopropyl-1-thio-b-D-galactopyranoside (IPTG; 40 μM) and ampicillin (Ap; 10 μg/ml) were added to media as necessary. All cultures were incubated at 37 °C. Biological F_1F_O ATP synthase activity was determined by

```
                              33        36         39 40                                                54
                           A  I  E  K   R  Q  K  E  I  A  D  G  L  A  S  A  E  R  A  H  K  D  L
pTAM46 (b_wt)       GCAATTGAAAAACGTCAAAAAGAAATTGCTGACGGCCTTGCTTCCGCAGAACGAGCACATAAGGACCT
                    MfeI                                                                      PpuMI

                                       E
pTAM54 (b_arg36→glu)     GCAATTGAAAAAGAGCAAAAAGAAATTGCTGACGGCCTTGCTTCCGCAGAACGAGCACATAAGGACCT
                                       E         R
pAW1 (b_arg36→glu,glu39→arg)  GCAATTGAAAAAGAGCAAAAACGAATTGCTGACGGCCTTGCTAGCGCAGAACGAGCACATAAGGACCT
                                       R         R              NheI
pAW5 (b_glu39→arg)       GCAATTGAAAAACGACAAAAACGAATTGCTGACGGCCTTGCTAGCGCAGAACGAGCACATAAGGACCT
                                                                NheI

                                       I
pTAM53 (b_arg36→ile)     GCAATTGAAAAAATACAAAAAGAAATTGCTGACGGCCTTGCTTCCGCAGAACGAGCACATAAGGACCT
                                       I          R
pAW4 (b_arg36→ile,ile40→arg)  GCAATTGAAAAAATACAAAAAGAGCGCGCTGACGGGCTAGCTTCCGCAGAACGAGCACATAAGGACCT
                                             BssHII         NheI
                           R           I
pAW6 (b_ile33→arg,arg36→ile)  GCGCGCGAAAAAATACAAAAAGAGATTGCTGACGGGCTAGCTTCCGCAGAACGAGCACATAAGGACCT
                           BssHII                        NheI
                                       I          R
pAW9 (b_arg36→ile,glu39→arg)  GCAATTGAAAAAATACAAAAACGAATTGCTGACGGCCTTGCTAGCGCAGAACGAGCACATAAGGACCT
                                                                NheI
```

Fig. 1 Sense strand sequences of recombinant *uncF(b)* genes. Top, the wild-type nucleotide sequence and deduced amino acid sequences of pTAM46 (b_{V5}) corresponding to amino acids 32–54 of the *b* subunit. Subsequent lines describe novel constructs. The plasmid name and mutation are noted on the *left*. Mutated nucleotides resulting in a change in the amino acid sequence are *bolded*, and restriction sites used for screening or mutagenesis purposes are *underlined* and labeled

streaking all strains onto plates containing a Minimal A media supplemented with 0.2% (w/v) succinate and incubated at either 37 or 25 °C.

Preparative procedures Inverted membrane vesicles were prepared from 500 ml cultures of LBG (Ap) medium containing 40 μM IPTG. Cells were harvested, washed twice with TM Buffer (50 mM Tris·HCl, 10 mM MgSO₄, pH 7.5), and then suspended in TM Buffer with 10 μg/ml DNaseI. Cells were broken using the French Press at 14,000 p.s.i. Unbroken cells were pelleted via two successive centrifugations at 9,000 rpm for 6 min each. Membranes were collected using ultracentrifugation at 48,000 rpm for 1.5 h in a Beckman 70.1 Ti rotor. Membranes were washed in TM buffer and pelleted using ultracentrifugation at 48,000 rpm for 1 h. The pellet was suspended in 1 ml TM buffer, centrifuged for 10 min at 13,000 rpm, and stored at 4 °C (Sorgen et al. 1998). Protein concentrations were determined using the modified Lowry assay for membrane proteins (Markwell et al. 1978). Growth on a plate with Minimal A media supplemented by 0.2% (w/v) succinate was used as an in vivo measure of enzyme viability.

Assay of F_1F_O ATP synthase activity Membrane energization was detected by fluorescence quenching of 9-amino-6-chloro-2-methoxyacridine (ACMA; Aris et al. 1985). This assay was performed using a Photon Technology International Fluorimeter and the associated Felix32 software. A time-based assay was performed for 720 s. The excitation and emission wavelengths were set at 410 and 490 nm, respectively. In a cuvette, 500 μg of protein was diluted in 3 ml MOPS buffer (50 mM MOPS, 10 mM MgCl₂, pH 7.3)

at 25 °C. At 30 s 15 μl of 0.2 mM ACMA was added to the cuvette. At 90 s 15 μl of 0.15 M ATP was added. The quenching of fluorescence was observed for the remaining 630 s.

Membrane-associated ATP hydrolysis activity was assayed using the acid molybdate method (Cain and Simoni 1989). A high pH buffer (50 mM Tris–HCl, 1 mM MgCl₂, pH 9.1) was used to relieve the effects of F_O on F_1. The reaction consists of 4 ml of pH 9.1 buffer, 60 μg protein, and 15 μl 0.15 M ATP (25 mM Tris–HCl, pH 7.5) at 37 °C. At specific time points, 218 μl of the reaction was taken out and placed in 1 ml iced stop buffer (9% HCl (v/v), 0.6% ammonium molybdate (v/v), 1.7% SDS (w/v). To each of these samples 100 μl of 10% solution of Eikongen (1.44 mM NaHSO₃, 95 μM Na₂SO₃, 10.45 μM 1-amino-2-naphthol-4-sulfonic acid) was added and incubated at 25 °C for 30 min. The absorbance at 700 nm was observed for each sample.

Immunoblot analysis Proteins (1.0 μg/well) were loaded onto a 15% Tris–glycine SDS BioRad Ready Gel. Following electrophoresis, the proteins were transferred onto a nitrocellulose membrane using electroblot (100 mV, 1 h, 4 °C). The membrane was washed three times with TBS (1 mM Tris–HCl, 15 mM NaCl pH 7.2). The proteins were then stained with Fast Green stain to confirm transfer to the membrane. The membrane was rinsed with Fast Green Destain and then washed three times with T-TBS (1 mM Tris–HCl, 15 mM NaCl pH 7.2 with 0.1% Tween-80, v/v). The membrane was incubated overnight at 4 °C in the presence of 5% dry non-fat milk in TBS. The membrane was then washed three times with T-TBS. Then,

a 1:4,000 dilution of the anti-V5 antibody in 2% BSA/T-TBS was incubated at 25 °C for 1 h. The membrane was washed three times in T-TBS and then incubated at 25 °C in a 1:20,000 dilution of the anti-mouse, horseradish peroxidase linked whole antibody, (from sheep). Following this incubation, the membrane was washed five times with T-TBS. The antibody was detected using chemiluminescence (ECL Plus, Amersham). The signals were visualized using high performance chemiluminescence film using a Kodak X-Omat. Signal strength was assessed using Un-Scan-It gel digitizing software (Silk Scientific, Inc.).

Results

Construction and growth characteristics of mutants Previous studies have shown that amino acid substitutions $b_{arg36\rightarrow ile}$ and $b_{arg36\rightarrow glu}$ were sufficient to inactivate F_1F_O ATP synthase (Caviston et al. 1998; Grabar and Cain 2004). Three double mutants were constructed with an isoleucine or glutamate at position 36 and the arginine residue replacing a naturally occurring glutamate or isoleucine. This segment of the *b* subunit is thought to be predominantly α-helical (Del Rizzo et al. 2002), so the positions of the amino acid replacements were designed to occur at one turn of the α-helix in either direction from b_{arg36} (Fig. 1). In addition, a single mutant was made, pAW5 ($b_{glu39\rightarrow arg\ V5}$), to consider whether two arginines in close proximity affected enzyme function. All plasmids were transformed into the *Escherichia coli* strain KM2 (Δ*b*), which contains a chromosomal deletion for the *uncF* (*b*) gene. This eliminated any endogenous *b* subunit

expression. The V5-epitope tag was engineered at the carboxyl terminus of the wild type and all mutant *b* subunits to facilitate detection of recombinant proteins. Previous reports have demonstrated that the V5 epitope tag has little effect upon enzyme assembly or activity (Grabar and Cain 2004).

First, the recombinant plasmids were tested for their ability to complement the deletion strain for growth on minimal A media supplemented with succinate. Since, F_1F_O ATP synthase is required for oxidative phosphorylation, growth on succinate as a carbon source served as an initial indication of the assembly of the mutant *b* subunits into functional enzyme. As expected, the single isoleucine mutant, KM2/pTAM53 ($b_{arg36\rightarrow ile\ V5}$), failed to grow on succinate (Caviston et al. 1998; Grabar and Cain 2004). Attempts to suppress the phenotype by using plasmids pAW4 ($b_{arg36\rightarrow ile,ile40\rightarrow arg\ V5}$) and pAW6 ($b_{ile33\rightarrow arg,arg36\rightarrow ile\ V5}$) were unsuccessful (Table 1).

However, a more interesting result was obtained for the $b_{arg36\rightarrow glu}$ mutant. The strain KM2/pTAM54 ($b_{arg36\rightarrow glu\ V5}$) did not grow on succinate. However, the first indication of suppression of an b_{arg36} defect appeared in the mutant strain, KM2/pAW1 ($b_{arg36\rightarrow glu,\ glu39\rightarrow arg\ V5}$) that grew slowly on succinate at 37 °C (Table 1). At 25 °C, the double mutant grew just as well as the wild-type control, KM2/pTAM46 (b_{V5}; Table 1). The results indicated that the $b_{arg36\rightarrow glu,glu39\rightarrow arg\ V5}$ subunit was functionally incorporated into an F_1F_O ATP synthase complex. Interestingly, addition of an arginine at position 39 yielded plasmid pAW5 ($b_{glu39\rightarrow arg\ V5}$) that also complemented strain KM2. However, it should be noted that strain KM2/pAW5 ($b_{glu39\rightarrow arg\ V5}$) grew more slowly than the wild-type control at either 37 or 25 °C (Table 1).

Table 1 Aerobic growth properties of mutants with double amino acid substitutions

Strains	Description	Growth[a]		Specific activity[b]	Wild type activity[c] (%)
		37 °C	25 °C		
KM2/pTAM46	b_{V5}, Ap^r	+++	+++	2.44±0.71	100
KM2/pBR322	Δ*b*, Ap^r	–	–	0.29±0.21	0.0
KM2/pTAM53	$b_{arg36\rightarrow ile\ V5}$, Ap^r	–	–	0.92±0.05	29
KM2/pTAM54	$b_{arg36\rightarrow glu\ V5}$, Ap^r	–	–	1.22±0.13	43
KM2/pAW1	$b_{arg36\rightarrow glu,\ glu39\rightarrow arg\ V5}$, Ap^r	++	+++	1.76±0.12	68
KM2/pAW4	$b_{arg36\rightarrow ile,\ ile40\rightarrow arg\ V5}$, Ap^r	-	-	1.18±0.10	41
KM2/pAW5	$b_{glu39\rightarrow arg\ V5}$, Ap^r	+	+	1.90±0.48	75
KM2/pAW6	$b_{ile33\rightarrow arg,\ arg36\rightarrow ile\ V5}$, Ap^r	–	–	1.47±0.19	55

[a] *E. coli* strains were grown aerobically on minimal A media supplemented with succinate. Colony size was scored after a 72-h incubation at either 37 or 25 °C as: +++, ≥1.0 mm; ++, 0.3–0.5 mm; –, no growth.
[b] ATPase activity was measured as described under "Experimental procedures." Units of specific activity = μmol PO_4 released mg^{-1} min^{-1} ± standard deviation. Units were calculated from the slope of the line based on six time points with incubations of 12 min. All values were performed in triplicate.
[c] Mutant activity less the activity of KM2/pBR322 divided by the activity of KM2/pTAM46 less the activity of KM2/pBR322 and converted to a percentage.
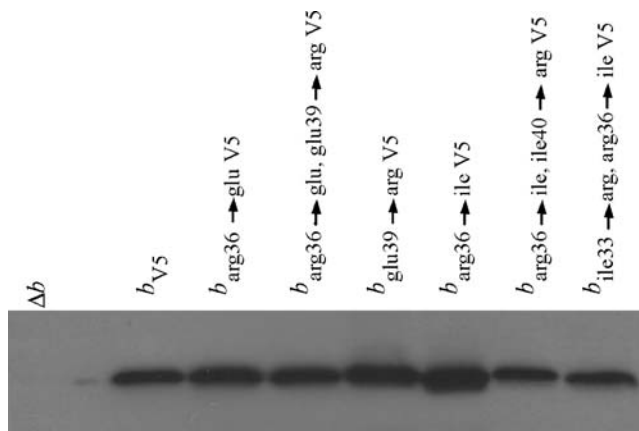
Fig. 2 Immunoblot analysis of *uncF*(*b*) gene mutant membranes. Membrane proteins were separated on a SDS gel and the proteins were transferred to nitrocellulose membranes (See "Experimental procedures"). The presence of *b* subunit was detected using an antibody against the V5 epitope tag located on the carboxyl terminus of the *b* subunits. *Lanes* Membranes prepared from strains: *1* KM2/pBR322, *2* blank, *3* KM2/pTAM46, *4* KM2/pTAM54, *5* KM2/pAW1, *6* KM2/pAW5, *7* KM2/pTAM53, *8* KM2/pAW4, *9* KM2/pAW6. Amino acid replacements in each subunit are specified above the *lanes*. Signal strengths on this and other blots were determined using a much shorter exposure and the Un-Scan-It gel digitizing software (Silk Scientific, Inc.)

Assembly of Intact F₁F_O ATP synthase Western blots were performed on membrane samples from the mutant strains using anti-V5 mouse monoclonal antibody to the mutant *b* subunits (Fig. 2). With IPTG included in the growth medium to achieve maximum production, the recombinant *b* subunits were found at levels comparable to control membranes. The
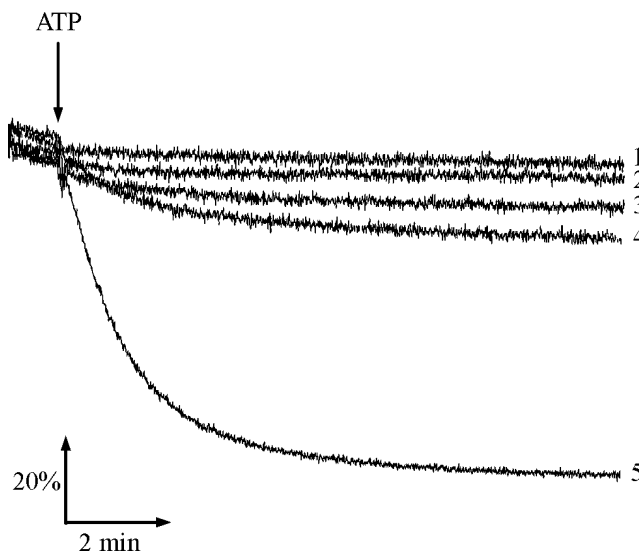
Fig. 3 ATP driven energization of membrane vesicles prepared from isoleucine *uncF*(*b*) gene mutants. Membranes from IPTG-induced strains were prepared by differential centrifugation (see "Experimental procedures"). Proton pumping was assayed using ACMA and 500 µg membrane protein. Traces: *1* KM2/pBR322 (Δb), *2* KM2/pAW4 ($b_{arg36\rightarrow ile, ile40\rightarrow arg\ V5}$), *3* KM2/pAW6 ($b_{ile33\rightarrow arg, arg36\rightarrow ile\ V5}$), *4* KM2/pTAM53 ($b_{arg36\rightarrow ile\ V5}$), *5* KM2/pTAM46 ($b_{V5}$)
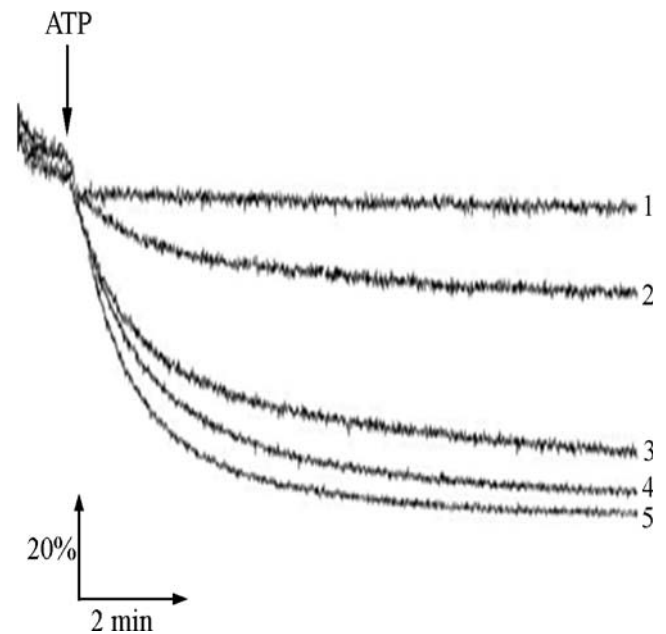
Fig. 4 ATP driven energization of membrane vesicles prepared from glutamic acid *uncF*(*b*) gene mutants. Membranes from IPTG-induced strains were prepared by differential centrifugation (see "Experimental procedures"). Proton pumping was assayed using ACMA and 500 µg membrane protein. Traces: *1* KM2/pBR322 (Δb), *2* KM2/pTAM54 ($b_{arg36\rightarrow glu\ V5}$), *3* KM2/pAW5 ($b_{glu39\rightarrow arg\ V5}$), *4* KM2/pAW1 ($b_{arg36\rightarrow glu, glu39\rightarrow arg\ V5}$), *5* KM2/pTAM46 ($b_{V5}$)

exceptions were membranes from strains KM2/pAW5 ($b_{glu39\rightarrow arg\ V5}$) and KM2/pTAM53 ($b_{arg36\rightarrow ile\ V5}$) that were expressed at levels approximately one and half times greater than the control KM2/pTAM46 (b_{V5}). The increased levels of these recombinant subunits were reproducible, and we have no explanation for the enhanced stability of the recombinant subunits. However, the important issue was that all recombinant *b* subunits were present, indicating that expression and incorporation into the membrane were not limiting for F₁F_O ATP synthase assembly.

In the absence of F_O, F₁ has very limited affinity for the membrane. Consequently, the level of F₁-ATPase activity was used as an indication of the amount of intact F₁F_O ATP synthase present in the sample. Assaying ATP hydrolysis at high pH relieves the influence of F_O on F₁, allowing for the measurement of maximal F₁-ATPase activity (Cain and Simoni 1989). All of the mutant strains yielded reduced levels of intact F₁F_O complexes (Table 1). The range for strains expressing *b* subunits with the $b_{arg36\rightarrow ile}$ substitution was between 30–55% of positive control values. The absolute numbers were somewhat higher than we have reported in the past reflecting improvements in procedures for washing and suspension of membrane vesicles. The levels of $b_{arg36\rightarrow glu}$ subunits also yielded reduced ATPase activity, at approximately 40–75% of the positive control. However, all recombinant *b* subunit membrane samples had ATP hydrolysis values substantially in excess of the
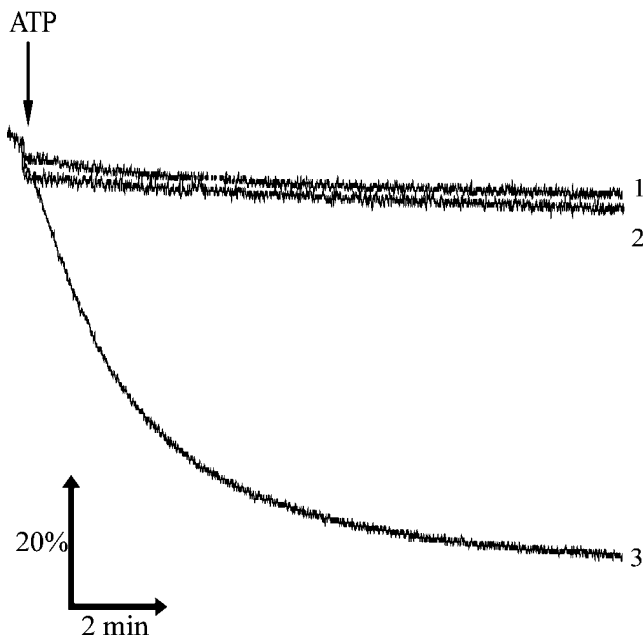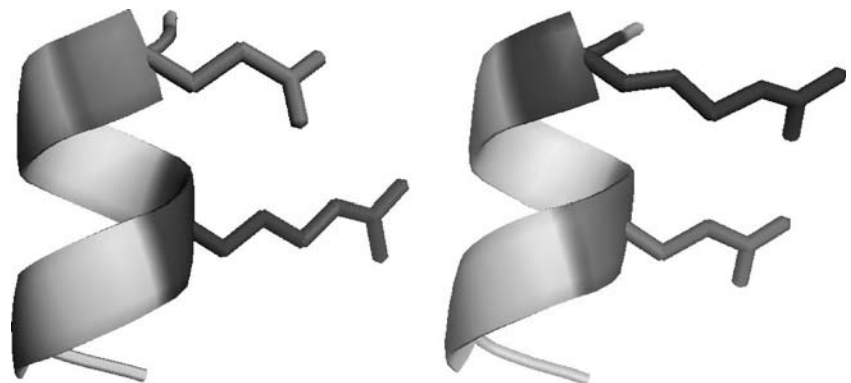
Fig. 5 ATP driven energization of membrane vesicles prepared from the $b_{arg36\rightarrow ile, glu39\rightarrow arg}$ V5 mutant. Membranes were processed as in Fig. 4 (see "Experimental procedures"). Traces: *1* KM2/pBR322 (Δb), *2* KM2/pAW9 ($b_{arg36\rightarrow ile, glu39\rightarrow arg}$ V5), *3* KM2/pTAM46 (b_{V5})

negative control KM2/pBR322 (Δb). The results suggested assembly of intact F_1F_O complexes containing the recombinant *b* subunits.

Coupled F_1F_O activity F_1F_O mediated ATP-driven proton pumping was determined as an indication of coupled activity in membrane vesicles. Earlier experiments showed reduced ATP driven membrane acidification in KM2/pTAM53 ($b_{arg36\rightarrow ile}$ V5) membranes (Caviston et al. 1998; Grabar and Cain 2004). However, a new PTI Q4SE fluorimenter with extended sensitivity and much-improved signal-to-noise ratio detected low levels of proton pumping activity (Fig. 3). There was no evidence that either KM2/pAW4 ($b_{arg36\rightarrow ile, ile40\rightarrow arg}$ V5) or KM2/pAW6 ($b_{ile33\rightarrow arg, arg36\rightarrow ile}$ V5) membranes had higher proton pumping activity than pTAM53 ($b_{arg36\rightarrow ile}$ V5; Fig. 3). However, very strong proton pumping activity was

observed in KM2/pAW1 ($b_{arg36\rightarrow glu, glu39\rightarrow arg}$ V5; Fig. 4). At this point it was apparent that positioning an arginine at residue 39 could suppress the $b_{arg36\rightarrow glu}$ mutation. A question then arose as to whether this $b_{glu39\rightarrow arg}$ substitution might also suppress the $b_{arg36\rightarrow ile}$ mutation. Therefore, another recombinant *b* subunit plasmid was constructed, plasmid pAW9 ($b_{arg36\rightarrow ile, glu39\rightarrow arg}$ V5). Although this mutant had adequate assembly, approximately 55% of that of wild-type, it did not exhibit any apparent ATP driven proton pumping (Fig. 5). This result suggested that $b_{glu39\rightarrow arg}$ suppression is specific for the $b_{arg36\rightarrow glu}$ mutation.

Discussion

Amino acid b_{arg36} is highly conserved and located in the tether domain in the immediate area of where the subunit emerges from the membrane bilayer. Amino acid substitutions for the conserved b_{arg36} have been shown to impair F_1F_0 ATP synthase by differing mechanisms. The $b_{arg36\rightarrow ile}$ substitution inhibited proton translocation in an intact F_1F_0 complex, and the $b_{arg36\rightarrow glu}$ uncoupled ion movement from catalytic activity (Caviston et al. 1998). Although extragenic suppression has been demonstrated between two *b* subunits in an F_1F_0 complex (Grabar and Cain 2004), the present work generated the first intragenic suppressor of a b_{arg36} substitution. No high-resolution structural information is available for the tether domain of the *b* subunit, but secondary structure predictions suggested that the area of the subunit containing b_{arg36} was likely to be α helical (Del Rizzo et al. 2002). Therefore, second site mutations were constructed to move the important arginine up or down one helical turn within the *b* subunit. The positions of arginine and isoleucine were swapped in the $b_{ile33\rightarrow arg, arg36\rightarrow ile}$ and $b_{arg36\rightarrow ile, ile40\rightarrow arg}$ subunits, and a similar inversion was made for the glutamate and arginine in the $b_{arg36\rightarrow glu, glu39\rightarrow arg}$ protein. Only expression of the latter recombinant subunit yielded an active F_1F_0 ATP synthase.

The $b_{arg36\rightarrow glu, glu39\rightarrow arg}$ subunit was readily incorporated into the F_1F_0 complex and yielded an essentially wild type

Fig. 6 Model of the b_{arg36} region in pTAM46 (b_{V5}) and in pAW1 ($b_{arg36\rightarrow glu, glu39\rightarrow arg}$ V5). An α-helical conformation was assumed based on secondary structure predictions. The model on the *left* shows residues 29 to 40 of the wild-type *b* subunit, with b_{arg36} shown in *black* and b_{glu39} in *gray*. The model on the right shows the same region of pAW1 ($b_{arg36\rightarrow glu, glu39\rightarrow arg}$ V5)

phenotype *in vivo*. The $b_{arg36\rightarrow glu}$ subunit uncoupled the enzyme (Caviston et al. 1998), and the double substitution was sufficient to effectively restore coupling. ATP-driven proton translocation in $b_{arg36\rightarrow glu, glu39\rightarrow arg}$ was greatly enhanced in comparison to $b_{arg36\rightarrow glu}$ substitution (Fig. 4). The evidence argues that the presence of the arginine is important for coupling, but it cannot be viewed as essential since several other substitutions exhibited at least partial function (Caviston et al. 1998). More specifically, a basic amino acid is needed for efficient coupling since the $b_{arg36\rightarrow lys}$ was almost fully functional (Caviston et al. 1998). A subunit with two tether domain arginines, $b_{glu39\rightarrow arg}$, was also incorporated into an active F_1F_0 ATP synthase (Table 1, Fig. 4). However, the mutant strain expressing the subunit grew poorly (Table 1). The result is reminiscent of the properties of the $b_{arg36\rightarrow glu}$ mutation, but with a much milder phenotype. It is possible that these mutations alter proton channel properties favoring an uncoupled phenotype.

However, it seems very unlikely that b_{arg36} substitutions alter interactions involved in the *b-b* dimer. Dimerization is governed by hydrophobic interactions at multiple positions along much of the length of the *b* subunit. An arginine contributed by each of the two *b* subunits would be expected to repel each other rather than strengthen the protein-protein interaction. Although there was an allusion to unpublished results showing disulfide bridge formation between $b_{gln37\rightarrow cys}$ subunits in a review article some years ago (Greie et al. 2000), no clear evidence has been reported of *b-b* subunit interactions in the tether domain between b_{gln10} and b_{ala59} (McLachlin and Dunn 1997; Dmitriev et al. 1999; Dunn et al. 2000, Greie et al. 2000). Involvement of b_{arg36} in an interaction with the *a* subunit offers a more reasonable interpretation. Chemical crosslinking has been reported between photoactivatable agents bound to $b_{arg36\rightarrow cys}$ and the *a* subunit (McLachlin et al. 2000). Another study showed crosslinking between $a_{lys74\rightarrow cys}$ in the first cytoplasmic loop of the *a* subunit and the tether domain of subunit *b* (Long et al. 2002). Although an interaction of the b_{arg36} with the *a* subunit appears likely, the exact role of b_{arg36} cannot be positively ascertained in the absence of more information about subunit interactions within F_0. However, the coupling defect observed in the original $b_{arg36\rightarrow glu}$ suggested either an opening of the *a* subunit proton channel or a loss of stator integrity. Normal function was recovered by reintroduction of an arginine into the tether domain in the $b_{arg36\rightarrow glu, glu39\rightarrow arg}$ subunit. Therefore, it is the presence of the arginine at a site low in the tether domain that is important. The length of the arginine side chain apparently facilitates positioning the guanidino group to perform its function (Fig. 6).

The presence of isoleucine at position 36 of the *b* subunit was apparently sufficient to prevent biologically significant levels of F_1F_0 ATP synthase activity. There was a significant assembly defect, and proton translocation was lost in fully assembled F_1F_0. Clearly, introduction of an arginine at a nearby second-site was not sufficient to restore measurable enzyme activity (Table 1, Figs. 3 and 5). Subunits containing the $b_{arg36\rightarrow ile}$ substitution do not have a productive interaction within the F_0 sector regardless of the presence of an additional arginine positioned in close proximity. Presumably the $b_{arg36\rightarrow ile}$ substitution results in an inappropriate conformation voiding *b* subunit function. The substitution does not materially affect the predicted propensity of the tether domain to form an α helix. However, the $b_{arg36\rightarrow ile}$ mutation phenotype was readily suppressed within an F_1F_0 complex containing a wild type *b* subunit (Grabar and Cain 2004). Therefore, it seems likely that it is an important intersubunit interaction between a single *b* subunit and the *a* subunit that has been disturbed.

The extraordinary degree of conservation of b_{arg36} among bacterial species has been documented (Caviston et al. 1998; Poetsch et al. 2007). However, the importance of a basic amino acid located in the *b* subunit near the membrane surface may extend to higher organisms, as well. With the exception of fungi, a lysine can be found at a comparable position in the mitochondrial *b* subunit from animals (Kim et al. 2004) and in subunit IV of plants (Poetsch et al. 2007). This information suggests that a basic amino acid contributes to efficient F_1F_0 ATP synthase coupling, not only in *E. coli* as evidenced by the $b_{arg36\rightarrow glu, glu39\rightarrow arg}$ double mutation, but in higher eukaryotes as well.

References

Aris JP, Klionsky DJ, Simoni RD (1985) J Biol Chem 260:11207–11215

Boyer PD (1993) Biochim Biophys Acta 1140:215–250

Boyer PD (2002) FEBS Lett 512:29–32

Cain BD (2000) J Bioenerg Biomembr 32:365–371

Cain BD, Simoni RD (1989) J Biol Chem 264:3292–3300

Caviston TL, Ketchum CJ, Sorgen PL, Nakamoto RK, Cain BD (1998) FEBS Lett 429:201–206

Del Rizzo PA, Bi Y, Dunn SD, Shilton BH (2002) Biochemistry 41:6875–6884

Dickson VK, Silvester JA, Fearnley IM, Leslie AG, Walker JE (2006) EMBO J 25:2911–2918

Dmitriev O, Jones PC, Jiang W, Fillingame RH (1999) J Biol Chem 274:15598–15604

Dunn SD, Revington M, Cipriano DJ, Shilton BH (2000) J Bioenerg Biomembr 32:347–355

Grabar TB, Cain BD (2004) J Biol Chem 279:31205–31211

Greie JC, Deckers-Hebestreit G, Altendorf K (2000) J Bioenerg Biomembr 32:357–364

Greie JC, Heitkamp T, Altendorf K (2004) Eur J Biochem 271:3036–3042

Hardy AW, Grabar TB, Bhatt D, Cain BD (2003) J Bioenerg Biomembr 35:389–397

Jones PC, Hermolin J, Jiang W, Fillingame RH (2000) J Biol Chem 275:31340–31346

Kim MS, Kim IC, Kim SS, Kim SK, Lee YM, Kang HS, Kweon HS, Hwang UW, Kim MK, Lee JS, Yoon YD (2004) DNA Seq 15:196–201

Leslie AG, Abrahams JP, Braig K, Lutter R, Menz RI, Orriss GL, van Raaij MJ, Walker JE (1999) Biochem Soc Trans 27:37–42

Long JC, DeLeon-Rangel J, Vik SB (2002) J Biol Chem 277:27288–27293

Markwell MA, Haas SM, Bieber LL, Tolbert NE (1978) Anal Biochem 87:206–210

McCormick KA, Cain BD (1991) J Bacteriol 173:7240–7248

McLachlin DT, Dunn SD (1997) J Biol Chem 272:21233–21239

McLachlin DT, Dunn SD (2000) Biochemistry 39:3486–3490

McLachlin DT, Bestard JA, Dunn SD (1998) J Biol Chem 273:15162–15168

McLachlin DT, Coveny AM, Clark SM, Dunn SD (2000) J Biol Chem 275:17571–17577

Motz C, Hornung T, Kersten M, McLachlin DT, Dunn SD, Wise JG, Vogel PD (2004) J Biol Chem 279:49074–49081

Ogilvie I, Aggeler R, Capaldi RA (1997) J Biol Chem 272:16652–16656

Poetsch A, Berzborn RJ, Heberle J, Link TA, Dencher NA, Seelert H (2007) J Biochem (Tokyo) 141:411–420

Revington M, McLachlin DT, Shaw GS, Dunn SD (1999) J Biol Chem 274:31094–31101

Senior AE, Nadanaciva S, Weber J (2002) Biochim Biophys Acta 1553:188–211

Sorgen PL, Caviston TL, Perry RC, Cain BD (1998) J Biol Chem 273:27873–27878

Sorgen PL, Bubb MR, Cain BD (1999) J Biol Chem 274:36261–36266

Stalz WD, Greie JC, Deckers-Hebestreit G, Altendorf K (2003) J Biol Chem 278:27068–27071

Stock D, Gibbons C, Arechaga I, Leslie AG, Walker JE (2000) Curr Opin Struct Biol 10:672–679